

Structural phase transition and ferromagnetism in monodisperse 3 nm FePt particles

Chuan-bing Rong, Narayan Poudyal, Girija S Chaubey, and Vikas Nandwana
Department of Physics, The University of Texas at Arlington, Arlington, Texas 76019

R. Skomski
*Center for Materials Research and Analysis, and Department of Physics and Astronomy,
 University of Nebraska, Lincoln, Nebraska 68588*

Y. Q. Wu and M. J. Kramer
*Ames Laboratory and Department of Materials Science and Engineering, Iowa State University, Ames,
 Iowa 50011*

J. Ping Liu^{a)}
Department of Physics, The University of Texas at Arlington, Arlington, Texas 76019

(Received 30 May 2007; accepted 12 July 2007; published online 30 August 2007)

FePt nanoparticles with a size of 3 nm and thermally stable room-temperature ferromagnetism are investigated. The monodisperse nanoparticles were prepared by chemical synthesis and a salt-matrix annealing technique. Structural and magnetic characterizations confirmed the phase transition from the disordered face-centered cubic structure to the $L1_0$ structure with the chemical ordering parameter of 0.62 ± 0.05 . Analysis in blocking temperature and fitting of temperature dependence of switching field reveals that the transformed 3 nm nanoparticles have a magnetic anisotropy constant of $(2.8 \pm 0.2) \times 10^6$ J/m³, smaller than those for the bigger particles and the fully ordered $L1_0$ bulk phase. © 2007 American Institute of Physics. [DOI: 10.1063/1.2773694]

I. INTRODUCTION

In light of the large magnetocrystalline anisotropy (7×10^6 J/m³), $L1_0$ -ordered FePt is ideal for the next generations of magnetic recording media and advanced permanent magnets.^{1–8} Chemically synthesized FePt nanoparticles have attracted tremendous attention since Sun *et al.*² reported their success in obtaining monodisperse nanoparticles. A key aspect of this technological development is to reduce the ferromagnetic particle size to 10 nm or less. In contrast, most other small magnetic particles are superparamagnetic at room temperature. Calculations predict that the high anisotropy of $L1_0$ FePt particles should lead to room-temperature ferromagnetic stability for particle sizes as small as 3 nm.^{9–11} Unfortunately, the as-synthesized nanoparticles take a disordered face-centered cubic (fcc) structure which has low magnetocrystalline anisotropy and cannot be applied as the recording media or permanent magnets. Annealing is necessary to convert the fcc phase to the ordered $L1_0$ phase with a tetragonal structure, yet these heat treatments always lead to reactive sintering. It was not until recently that monodisperse FePt nanoparticles with the $L1_0$ structure have been available by salt-matrix annealing, which enables us to study the size effect on the magnetic properties of the FePt material.^{8,12}

Coincidentally, there is another critical size of about 3 nm, related to FePt nanoparticles. It has been reported recently that when particle size of FePt nanoparticles is smaller than 3 nm, the fcc- $L1_0$ phase transition will be suppressed.¹³ Furthermore, the equilibrium behavior of the nanoparticles is only partially understood. Experiments on isolated granular

thin films¹⁴ and monodisperse nanoparticles^{8,12} have shown that the phase transition from fcc to $L1_0$ occurs when particle size is larger than 4 nm but did not occur when the particle size is 2 nm. It is therefore curious to see structural and magnetic properties of 3 nm FePt particles. In this work, we report the preparation, structural phase transition, and magnetic characterizations of heat-treated monodisperse FePt nanoparticles of 3 nm size.

II. EXPERIMENT

The 3 nm FePt nanoparticles with fcc structure were prepared via chemical reduction of Pt(acac)₂ and thermal decomposition of Fe(CO)₅ in the presence of oleic acid and oleyl amine, which is similar to the preparation of 4 nm FePt nanoparticle as presented in Ref. 2. The difference is that the molar ratio of surfactants to Pt(acac)₂ is 3/4 for 3 nm instead of 1/1 for 4 nm. The fcc nanoparticles were then transformed to $L1_0$ nanoparticles with no particle growth using the salt-matrix annealing technique, with salt/sample mass ratio around 400:1.¹² The heat treatments were carried out at 700 °C for 4 h, which is considered sufficient for the ordering phase transition. Tecnai G² F20 scanning transmission electron microscope (STEM) was operated at 200 kV to analyze the morphology and crystalline structures. The composition of nanoparticles (around Fe₅₄Pt₄₆) was checked by energy dispersive x-ray (EDX) analysis. X-ray diffraction (XRD) was used to determine phase transition, the long-range ordering parameters, and the grain size or particle size. The magnetic hysteresis loops were measured with a magnetic properties measurement system (MPMS) from specimens of mixture of epoxy and the magnetic nanoparticles.

^{a)}Electronic mail: pliu@uta.edu

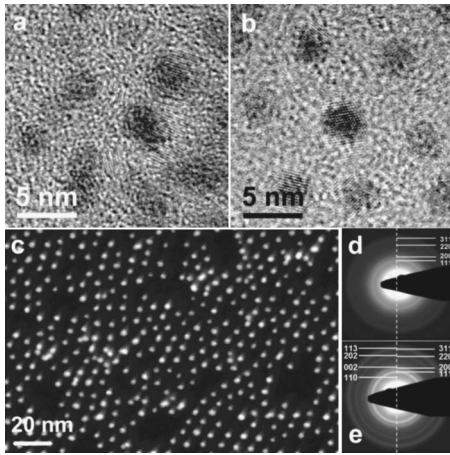


FIG. 1. TEM analysis of the 3 nm FePt nanoparticle before and after salt-matrix annealing: (a) and (b) HRTEM images of the particles before and after salt-matrix annealing, respectively; (c) STEM HDAAF image of the annealed particles; (d) and (e) SAED patterns of the particle before and after annealing, respectively.

III. RESULTS AND DISCUSSION

Figures 1(a) and 1(b) show the high-resolution TEM images of the 3 nm FePt nanoparticles before and after annealing in a salt matrix at 700 °C for 4 h, respectively. It can be seen that the particle sizes are retained after the annealing. Both the as-synthesized and annealed nanoparticles are monodisperse with a standard deviation of about 5–10% in diameter, which is based on more than 100 particles from the high-resolution TEM images. A large-region STEM high-angle annular dark field (HAADF) image [Fig. 1(c)] also shows no sintering of the annealed particles. To check the phase transition by salt-matrix annealing, the selected area electron diffraction (SAED) patterns were obtained for the particles before and after annealing. The SAED patterns indicate that the as-synthesized and annealed nanoparticles are fcc and $L1_0$ phase, respectively, as shown in Figs. 1(d) and 1(e).

The XRD patterns in Fig. 2 confirm that the annealing in the salt matrix transforms the disordered fcc structure into

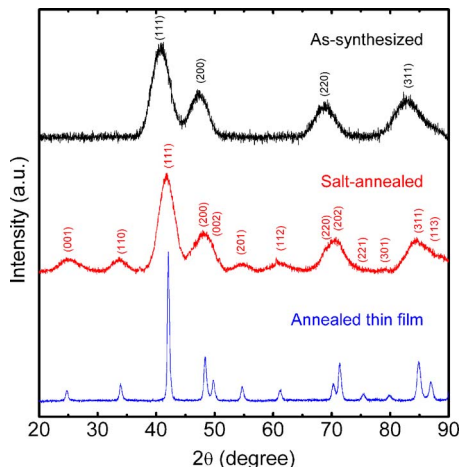


FIG. 2. (Color online) XRD patterns of the FePt nanoparticles before and after salt-matrix annealing. The pattern of the annealed film, which is made from the 3 nm nanoparticles, is also included for comparison.

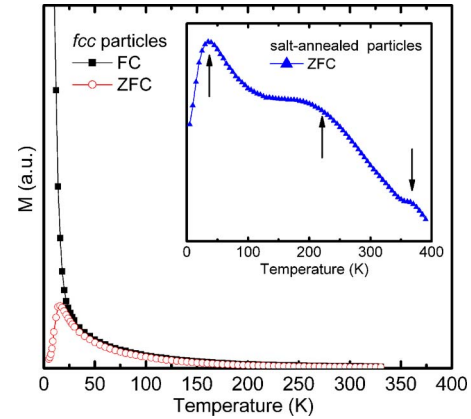


FIG. 3. (Color online) ZFC and FC curves of as-synthesized nanoparticles. The inset gives the ZFC curve of salt-annealed particles.

the tetragonal $L1_0$ structure. Figure 2 also gives the XRD pattern of the FePt film, which was obtained by dropping the nanoparticles on Si wafer and traditional annealing at 700 °C for 1 h without salt matrix. The annealed grain size was estimated to be around 30 nm based on the sharpening of the XRD pattern. To detect the degree of structural ordering of the $L1_0$ particles, the chemical ordering parameter S was calculated by

$$S = \left[\left(\frac{I_{001}}{I_{002}} \right) \times \left(\frac{F_f}{F_s} \right)^2 \frac{(L \times A \times D)_f}{(L \times A \times D)_s} \right]^{1/2} \cong 0.85 \left[\frac{I_{001}}{I_{002}} \right]^{1/2}, \quad (1)$$

where I_{hkl} , F , L , A , and D are the integrated intensity, structure factor, Lorentz polarization factor, absorption factor, and temperature factor, respectively. Subscripts f and s indicate values for the fundamental and the superlattice reflections, respectively.^{8,15,16} S of the 3 nm annealed particles is 0.62 ± 0.05 by the above formula. The error is estimated by the standard deviation based on four independent XRD measurements. It should be noted that S is only measured from the ordered or partially ordered particles since the disordered particles do not have both the superlattice (001) and fundamental (002) reflections which were used to calculate S by Eq. (1). It was found that S of the 3 nm $L1_0$ particles is lower than that of 4 nm $L1_0$ particles, which is around 0.78,⁸ indicating an incomplete phase transition in the smaller particles. The low observed S may be caused by the difficulties to achieve equilibrium state due to slow kinetic process for small particles.¹³

Figure 3 shows the zero-field cooled (ZFC) and field-cooled (FC) curves of the as-synthesized nanoparticles. The blocking temperature (T_B) of the fcc nanoparticles, which is determined from the maximum of the ZFC curve, is around 15 K. It is interesting to find that there is one peak and two inflections in the ZFC curve of the salt-matrix annealed nanoparticles (as shown in the inset of Fig. 3). The peak around 35 ± 5 K should be the blocking temperature (T_{B1}) of the disordered (and/or partly ordered) nanoparticles, which is higher than that of totally disordered fcc nanoparticle before annealing. The two inflections therefore are T_B of the ordered $L1_0$ nanoparticles, which are around $T_{B2} = 222 \pm 20$ K, $T_{B3} = 363 \pm 10$ K, respectively. Here, T_B was determined from

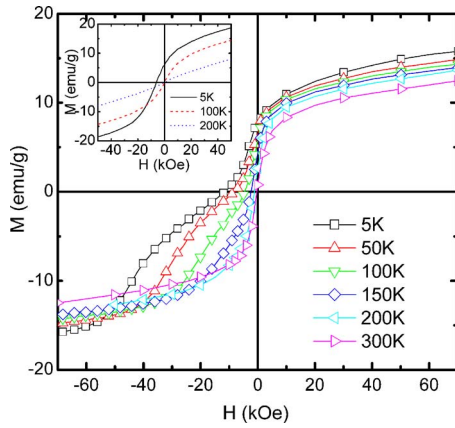


FIG. 4. (Color online) Hysteresis loops of the salt-annealed at different temperature. The inset shows the hysteresis loops of the fcc nanoparticle before annealing.

the intersections of extrapolations of the greatest slope and flat region. Assuming $K_u V / (k_B T_B) \approx 25$ for a random distribution of particles with a single magnetic domain,¹⁷ the values of effective anisotropy K_u are estimated to be $(0.45 \pm 0.06) \times 10^6$, $(2.84 \pm 0.26) \times 10^6$, and $(4.70 \pm 0.13) \times 10^6$ J/m³ for the 3 nm particles with different T_B . Here, V and k_B are the average particle volume and Boltzmann constant, respectively. On the other hand, if we assume K_u of the particle with T_{B3} is fixed at $(2.84 \pm 0.26) \times 10^6$ J/m³, the particle size of T_{B3} is estimated around 3.5 ± 1.1 nm. Therefore, it is reasonable to assume that K_u is around $(2.84 \pm 0.26) \times 10^6$ J/m³ for the ordered 3 nm particles. This value is lower than that of bulk phase (7×10^6 J/m³) and even lower than that of 3.5 nm $L1_0$ FePt nanoparticles (4.96×10^6 J/m³) embedded in carbon matrix.¹⁸ The relatively low K_u implies again an incomplete phase transition in the 3 nm particles.

Figure 4 shows the hysteresis loops of the annealed nanoparticles at different temperatures. The magnetization curves show large kinks, which indicate that the nanoparticles mainly consist of two phases, essentially $L1_0$ and fcc phases. We use the corresponding susceptibility maxima to define two switching fields (H_s) of the two phases, H_s^1 belonging to the ordered $L1_0$ nanoparticles, and $H_s^2 < H_s^1$ describing the disordered fcc or partially ordered particles. It is interesting to note that the annealed nanoparticles are ferromagnetic at room temperature. However, the fcc nanoparticles have a coercivity of only 6 kOe at 5 K and then become superparamagnetic when the temperature is higher than 15 K (as shown in the inset of Fig. 4). These results are consistent with the ZFC analysis.

As discussed above, the annealed 3 nm nanoparticles have a distribution of anisotropy field which may be caused by the composition or size distribution of the particles. Magnetic phase analysis based on Stoner-Wohlfarth¹⁹ hysteresis loops for an ensemble of isotropic noninteracting small particles makes it possible to describe the nanoparticles by a weight function $g(H_s)$, since H_s of the Stoner-Wohlfarth particles is half of the anisotropy field. The statistic analysis shows that the magnetization behavior is equivalent to a system consisting of a mixture of 64% ordered particles with

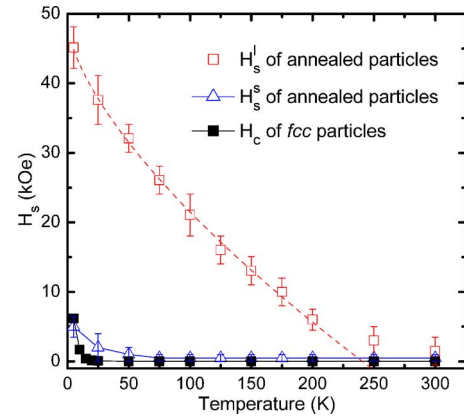


FIG. 5. (Color online) Temperature dependence of switching field H_s^1 and H_s^2 of the annealed 3 nm nanoparticles and the coercivity of the as-synthesized particles. The dashed line is the Kneller-Sharrock fitting of the H_s^1 data.

uniaxial anisotropy, 11% partially ordered, and 25% disordered fcc particles if we consider that the ordered and disordered particles have switching fields larger than 30 kOe and smaller than 7 kOe at 5 K, respectively. One should note that there is no direct correlation between the percentage 75% of the transformed particles and the chemical ordering parameter S of 0.62. Actually, $S=0.62$ was only measured from the 75% ordered and partially ordered particles. Although the phase transition from fcc to $L1_0$ structure in thin films can be explained by the nucleation mode,^{20,21} the physical nature of the partial ordering in the FePt nanoparticles suggested by our magnetic and characterization experiments is still unclear. Possible explanations are a bimodal distribution (coexistence of ordered and disordered particles) of ordered and disordered regions in each particle.²²

Figure 5 gives the temperature dependence of H_s of the salt-matrix annealed nanoparticles. The open squares and triangles represent H_s^1 and H_s^2 , respectively. For comparison, the coercivity of the fcc nanoparticle before annealing is also given in Fig. 5 (solid squares). It shows that the temperature dependence of H_s^1 is similar to that of the coercivity of fcc nanoparticles, which confirms that the particles with H_s^1 are not transformed. The transformed particles show high switching field above 6 kOe when the temperature is lower than 200 K. However, H_s^1 drops significantly with increasing temperature. This is mainly due to the strong thermal activation effects in the nanoparticles, which can be approximated by the Kneller-Sharrock formula.^{23,24} The fitting of temperature-dependent H_s^1 gives $H_0=48.5$ kOe and $K_u = (2.77 \pm 0.21) \times 10^6$ J/m³, which agrees well with the ZFC analysis. Note that K_u of $L1_0$ FePt phase is weakly temperature-dependent, so that the curve fitting thus can be done with the temperature range between 10 to 200 K.²⁵

IV. CONCLUSION

Monodisperse 3 nm fcc nanoparticles have been prepared by chemical synthesis. The fcc particles underwent salt-matrix annealing at 700 °C for 4 h, which is considered to be sufficient for the fcc- $L1_0$ phase transition. The structural and magnetic analyses show that after the annealing the majority of the particles transformed to the ordered $L1_0$

phase, while a small portion of the particles remained disordered. The ordered particles have a relatively low chemical ordering parameter compared to large particles. The fitting of magnetization data using a Stoner-Wohlfarth model gives quantitative distribution that 64% of the annealed particles are ordered $L1_0$ particles. For the ordered 3 nm particles, the zero-field cooled (ZFC) magnetization and the temperature dependence of the switching field yield an anisotropy constant of around 2.8×10^6 J/m³. This anisotropy is substantial but somewhat smaller than the bulk anisotropy, reflecting a partial ordering in the very small particles.

ACKNOWLEDGMENTS

This work was supported by U.S. DoD/MURI Grant N00014-05-1-0497 and DARPA through ARO under Grant No DAAD 19-03-1-0038. Work at the Ames Laboratory was supported by the Department of Energy-Basic Energy Sciences under Contract No. DE-AC02-07CH11358. Work at the University of Nebraska was supported by NSF-MRSEC and NCMN.

- ¹J. P. Liu, Y. Liu, C. P. Luo, Z. S. Shan, and D. J. Sellmyer, *J. Appl. Phys.* **81**, 5644 (1997).
- ²S. Sun, C. B. Murray, D. Weller, L. Folks, and A. Moser, *Science* **287**, 1989 (2000).
- ³H. Zeng, J. Li, J. P. Liu, Z. L. Wang, and S. H. Sun, *Nature* **420**, 395 (2002).
- ⁴S. Okamoto, O. Kitakami, N. Kikuchi, T. Miyazaki, Y. Shimada, and Y. K. Takahashi, *Phys. Rev. B* **67**, 094422 (2003).
- ⁵C. B. Rong, H. W. Zhang, X. B. Du, J. Zhang, S. Y. Zhang, and B. G. Shen, *J. Appl. Phys.* **96**, 3921 (2004).
- ⁶J. W. Harrell, S. Kang, Z. Jia, D. E. Nikles, R. Chantrell, and A. Satoh,

- Appl. Phys. Lett.* **87**, 202508 (2005).
- ⁷J. M. Qiu, J. M. Bai, and J. P. Wang, *Appl. Phys. Lett.* **89**, 222506 (2006).
- ⁸C. B. Rong, D. R. Li, V. Nandwana, N. Poudyal, Y. Ding, Z. L. Wang, H. Zeng, and J. P. Liu, *Adv. Mater.* **18**, 2984 (2006).
- ⁹D. Weller, A. Moser, L. Folks, M. E. Best, W. Lee, M. F. Toney, M. Schwickert, J. U. Thiele, and M. F. Doerner, *IEEE Trans. Magn.* **36**, 10 (2000).
- ¹⁰R. Skomski and J. M. D. Coey, *Permanent Magnetism* (Institute of Physics, Bristol, 1999).
- ¹¹*Advanced Magnetic Nanostructures*, edited by D. J. Sellmyer and R. Skomski (Springer, Berlin, 2006).
- ¹²K. Elkins, D. Li, N. Poudyal, V. Nandwana, Z. Jin, K. Chen, and J. P. Liu, *J. Phys. D* **38**, 2306 (2005).
- ¹³R. V. Chepurskii and W. H. Butler, *Phys. Rev. B* **72**, 134205 (2005).
- ¹⁴T. Miyazaki, O. Kitakami, S. Okamoto, Y. Shimada, Z. Akase, Y. Murakami, D. Shindo, Y. K. Takahashi, and K. Hono, *Phys. Rev. B* **72**, 144419 (2005).
- ¹⁵B. E. Warren, *X-Ray Diffraction* (Dover, New York, 1990), Chap. 12.
- ¹⁶J. A. Christodoulides, P. Farber, M. Daniil, H. Okumura, G. C. Hadjipanayis, V. Skumryev, A. Simopoulos, and D. Weller, *IEEE Trans. Magn.* **37**, 1292 (2001).
- ¹⁷M. El-Hilo, K. O'Grady, and R. W. Chantrell, *J. Magn. Magn. Mater.* **114**, 295 (1992).
- ¹⁸S. Momose, H. Kodama, N. Ihara, T. Uzumaki, and A. Tanaka, *Jpn. J. Appl. Phys., Part 1* **42**, L1252 (2003).
- ¹⁹E. C. Stoner and E. P. Wohlfarth, *Philos. Trans. R. Soc. London, Ser. A* **240**, 599 (1948).
- ²⁰K. Barmak, J. Kim, S. Shell, E. B. Svedberg, and J. K. Howard, *Appl. Phys. Lett.* **80**, 4268 (2002).
- ²¹D. C. Berry and K. Barmak, *J. Appl. Phys.* **101**, 014905 (2007).
- ²²S.S. Kang, S.F. Shi, Z.Y. Jia, G.B. Thompson, D. E. Nikles, J.W. Harrell, D. Li, N. Poudyal, V. Nandwana, and J. P. Liu, *J. Appl. Phys.* **101**, 09J113 (2007).
- ²³E. Kneller, in *Handbuch der Physik XIII/2: Ferromagnetismus*, edited by H. P. J. Wijn (Springer, Berlin, 1966), pp. 438–544.
- ²⁴M. P. Sharrock, *J. Appl. Phys.* **76**, 6413 (1994).
- ²⁵S. Okamoto, N. Kikuchi, O. Kitakami, T. Miyazaki, Y. Shimada, and K. Fukamichi, *Phys. Rev. B* **66**, 024413 (2002).